UNIVERSITAT POLITÈCNICA
DE CATALUNYA
BARCELONATECH

UPCommons

Portal del coneixement obert de la UPC

http://upcommons.upc.edu/e-prints

Aquesta és una còpia de la versió *author's final draft* d'un article publicat a la revista *Journal of materials processing technology*.

URL d'aquest document a UPCommons E-prints:
http://hdl.handle.net/2117/127903

Article publicat / *Published paper*:

Gómez-Monterde, J., Hain, J., Sánchez-Soto, M., Maspoch, M.Ll. (2019) Microcellular injection moulding: a comparison between MuCell process and the novel micro-foaming technology IQ Foam. Journal of materials processing technology, vol. 268, p. 162-170.
Doi: 10.1016/j.jmatprotec.2019.01.015

***Manuscript**
Click here to view linked References

Microcellular injection moulding: a comparison between MuCell process and the novel micro-foaming technology IQ Foam

J. Gómez-Monterde[a,]*, J. Hain[b], M. Sánchez-Soto[c], M. Ll. Maspoch[c]

[a] SEAT SA, Martorell, E-08760, Spain

[b] Volkswagen AG, Wolfsburg D-38436, Germany

[c] Centre Català del Plàstic, Universitat Politècnica de Catalunya-BarcelonaTech, Terrassa, E-08222, Spain

*Corresponding author:

Javier Gómez-Monterde (E-mail: javier1.gomez@seat.es / Telephone: +34 93 773 11 13)

ABSTRACT

The present work aims to compare two different injection moulding foaming technologies, the already known MuCell® process and the new emerged technology IQ Foam®, as well as the cell structure and mechanical behavior of the obtained components. Glass fiber reinforced-polypropylene (>PP GF<) was employed to produce rectangular plates at solid and foamed conditions by using MuCell® and IQ Foam® processes combined with the complementary Core Back expansion molding technology, and the material structure as well as the tensile, flexural and impact properties were studied.

A solid skin-foamed core structure was observed in the samples foamed by both techniques. The mechanical properties decreased gradually with the apparent density of the microcellular plates. By increasing the thickness of the part because of the expansion of the cavity with the Core Back technology, the apparent density decreased but the flexural stiffness was greatly enhanced. Foamed samples obtained by IQ Foam® technology exhibited thicker solid surface layers and lower cell density than that of the MuCell® ones, but consequently higher resistant area, and thus, slightly higher mechanical properties. The new IQ Foam® technology is able to produce foamed parts with properties comparable to that of the MuCell® process, offering additional benefits such as cost-effectiveness, easy to use and machine-independence.

Keywords: Microcellular injection molding; Plastic foams; Polypropylene-glass fibers

1. INTRODUCTION

Lightening of materials and products is a constant objective in the sectors of the economy as a way to reduce cost and energy. Due to their wide range of properties and intrinsic low density, polymers have acquired a predominant role in many industrial applications. Plastics are generally cost effective materials providing high design freedom to engineers. Moreover, they can be formulated in different ways, blended and reinforced with fillers, so that their properties can vary in a wide range of stiffness, softness and hardness, and offer the possibility to be formed into almost any shape, size or color. The above mentioned reasons explain that the demand of plastics for automotive applications has been constantly grown since 1970s until now, as has been pointed out by Inc (2012). Regulatory constraints and the increase in the environmental awareness make the automotive industry take different strategies to reduce greenhouse gas emissions and air pollutants, such as lightweight construction. Therefore, it seems appropriate to conduct strategies to make plastic parts lighter. One approach is to introduce a gas to remove part of the previously injected polymer. This process has been used to reduce weight and cycle time in the manufacturing of thick components (Sánchez-Soto et al., 2006). However, foaming techniques in which the gas expand in the mold inside the polymer melt, is nowadays considered as one of the most powerful methods to reduce weight in components made of plastic materials.

Out of the automotive industry, recent research on physical foaming of plastics has focused on many other fields. Conductive polymer composite foams for replacing metal-based electromagnetic interference shields have been developed with microcellular polystyrene (Min et al., 2018), poly (l-lactic acid) (Kuang et al., 2016) and polyethylene (Hamidinejad et al., 2018b). Hamidinejad et al. (2018a) showed an increase in the real permittivity and decrease in the dielectric loss with microcellular high-density polyethylene nanocomposites employed as dielectric materials for high-performance capacitors. It was also demonstrated by Kuang et al. (2018) that the introduction of foaming technique in poly (butylene succinate) (PBS)/carbon fiber (CF) composites could be beneficial for the formation of effective 3D conductivity networks, keeping good compressive strength. Kuang et al. (2017b) has also worked on improving the foaming ability of poly (propylene carbonate) (PPC) biocomposites to expand potential commercial applications without sacrificing their outstanding biodegradability. Open-cellular PLLA scaffolds foams with high porosity and excellent compressive stress has been easily prepared as substitutes for tissue engineering (Kuang et al., 2017a).

The microcellular injection molding MuCell® process consists of injecting a gas at supercritical state into the molten polymer (generally carbon dioxide or nitrogen) and allowing it to expand and fill the tool cavity, creating a cellular structure inside the part. Consequently, lighter components with improved dimensional stability are obtained. In addition, other advantages can be achieved through this process such as the decrease in the cost of foamed parts due to saved material and reduced cycle time and holding pressure because of the expanding force of the gas, as remarked by Handschke and Mitzler (2012). Some authors like Kim and Wallington (2013) as well as Elduque et al. (2014) also showed that microcellular injection molding allows not only to make industrial parts lighter, but also reduce carbon footprint and CO_2 emissions.

Nevertheless, the application of the MuCell® foaming technology has not been widely extended in automotive parts due to several factors. For example, the high initial investment to implement the process, the additional complexity in controlling the production and the lower mechanical properties and worse surface qualities of foamed components as compared to the solid counterpart. With the aim of overcoming some of these drawbacks, new foaming injection molding technologies have emerged, such as IQ Foam®, recently developed by Volkswagen AG.

The present work deals with the characterization of microcellular thermoplastic composites obtained by injection molding, as a preliminary approach towards lighter, cheaper and more environmentally plastic parts. A comparison between MuCell® and IQ Foam® foaming injection molding technologies is presented, in terms of morphology and tensile, flexural and impact properties of microcellular parts resulted from both processes. Moreover, the effect of mold cavity expansion through the Core Back tool technology on the foaming behavior is also studied.

2. BACKGROUND

Among the different technologies for foaming through injection molding developed, this study focuses on and compares two different processes: MuCell®, the most extended technology in the market, and IQ Foam®, a new microcellular process recently developed. Both foaming technologies were also employed with the Core Back complementary tool process. The operating principles of these techniques are discussed below.

2.1. MuCell® technology

The microcellular injection molding MuCell® process was developed by the Massachusetts Institute Technology (MIT) in the 1990s and since then it is licensed and commercialized by Trexel Inc (Pierick et al., 2005; Pierick et al., 1999). Among the different processes available for foaming thermoplastic materials, MuCell® has had the most industry acceptance and nowadays is the leading microcellular foaming technology. The fundamentals of MuCell® process consist basically of dissolving a blowing agent under supercritical conditions (SCF) in the molten polymer at the plasticizing unit, forming a single-phase solution. The pressure drops inducing cell nucleation and growth occurs at the entrance of the mold, so foaming takes place inside the mold cavity.

As illustrated in Figure 1, applying MuCell® involves new equipment and modifications in reference to conventional injection molding. On one hand, a gas, usually N_2 or CO_2, is raised to supercritical conditions in the SCF metering unit and conducted to the interface kit. It regulates the mass flow and provides the blowing agent when required. One or more gas injectors introduce the supercritical fluid in the barrel during the plasticizing stage. Opening and closing of gas injectors are controlled by time or screw position signals.

On the other hand, with the objective of homogenizing and stabilizing the single-phase solution, a special reciprocating screw is required. This screw is longer than a conventional one and equipped with a mixing section specially designed for optimizing the polymer/gas mixture. Back and front check valves prevent from expansion of the mixture towards the feeding zone and the nozzle, respectively. Regarding control of the process, additional aspects must be considered. When the blowing agent is injected in the plasticizing unit, the pressure drops from the supercritical state to the melt pressure. A supplementary variable, named Microcellular Plasticizing Pressure (MPP) measures the pressure of the system in the cylinder. The pressure drop between the gas injector and the MPP has to be limited, in order to avoid foaming inside the barrel. Xu (2010) provided a wide-ranging analysis of the influence of the processing parameters on the cell structure and properties, where injection rate, supercritical fluid dosing and content, tool temperature and shot size were determined as the most influential ones. According to preliminary studies made on ABS material (Gómez- Monterde et al., 2018), it was found a major effect of shot volume on the morphology, surface roughness and tensile characteristics, while the mold temperature and injection speed had a minor impact on these foam properties. The foamability of biodegradable polymers with narrow processing window and lower environmental impact, like PLA, has been also investigated (Pantani et al., 2014).

The advantages offered by MuCell® have been listed before, and include, weight reduction, improved dimensional stability, energy and clamping force decrease and cycle time shortening. However, the main limitation of the MuCell® is the economic investment needed to purchase the supercritical fluid supply system, as well as the special reciprocating screw. Other problems inherent to any gas foaming process are the worse surface quality and deterioration of mechanical properties.

2.2. IQ Foam® technology

IQ Foam® has been recently developed and it is expected to be integrated in industrial production in forthcoming years. It was conceived and patented by Volkswagen AG (Schütz et al., 2015) with the aim of reducing complexity and cost as compared to other available processes. The main equipment consists of a two-chambered unit assembled between the hopper and the feed of any conventional injection molding machine (Figure 2), where polymer is impregnated with gas before melting. This unit contains two gas injectors to introduce the physical blowing agent, valves to regulate the flow of gas and two actuators to allow polymer pellets to pass through the unit and to lock each chamber.

The operating principle of IQ Foam® is as follows (Figure 3):

1. Initially, both actuators close the chamber and there is no communication between the hopper and the feeding zone of the plasticizing unit. Polymer pellets stay in the hopper, and chambers are free of blowing agent.
2. Actuator 1 operates and pellets drop from the hopper to the upper chamber at ambient pressure. Then, the upper chamber is closed again by the actuator 1.
3. A gas injector introduces the gas into the upper chamber under low pressure. Usually, N_2 and CO_2 although it can work with any other physical blowing agent.

4. Actuator 2 opens the air lock between both chambers. The polymer falls into the lower chamber, the gas fills all the available space and the lower chamber locks again.
5. Remaining gas in upper chamber is re-routed to the lower one. A second injector adds gas to keep the desired pressure, ensuring gas moving forward with polymer pellets and diffuses during the plasticizing process. The upper chamber opens and refills again, and the cycle is repeated.

As described by Hain (2015), it is worth to notice that gas is supplied under moderate-low pressure directly from the bottle, without requiring gas-metering equipment. Re-routing gas from upper to lower chambers prevents from gas leakage and maximizes its use. The only important modification of the injection machine is sealing the back of the screw to avoid gas escaping. On the other hand, the foaming process can be controlled only by the gas pressure, so it can be easily automated and driven by an electronic system managing actuators and gas injectors regardless the original software control of the injection molding machine. Consequently, IQ Foam® arises as a potentially cost-effective and machine-independent process, easy to start up and reducing both weight and cost of plastic products significantly.

2.2. Core Back technology

Despite the many advantages of microcellular plastics listed above, it has been also reported some limitations, like mechanical properties deterioration and poor surface quality. Different technologies concerning the tool have been introduced to improve the quality of foamed polymers, like the Core Back expansion molding. It is a complementary tool technology able to improve surface quality, but also increase density reduction, stiffness-to-weight ratio and save weight in foamed thermoplastic parts. First, the cavity is volumetrically filled close to solid weight by polymer/gas mixture. The cavity is filled at high injection speed, so as to prevent pressure drop and foaming. After a delay time within which a solid skin is formed, the cavity is expanded and the increase in volume induces a sudden pressure drop, promoting foam generation inside the part. As the thickness increases, lower densities are reached. The entire cavity can be expanded, or only partially in determined areas of interest. Either way, precision machinery to move the mold components is required.

3. MATERIALS AND METHODS

3.1. Material and processing conditions

In this study a polypropylene reinforced with 20% of glass fibers (PP 20GF Fibremod™ GE277Al) was used. The density of the compound is 1.04 g cm^{-3} and the MFI 12 g 10 min^{-1}, and it is supplied by Borealis AG (Germany).

The PP 20GF material was previously dried at 80 ºC for at least 3 hours, as recommended by the supplier. Rectangular plates of 400x130 mm^2 (Figure 4a) and variable thickness were injection molded through MuCell® and IQ Foam® processes, combined with the Core Back technology. First, solid and foamed 3 mm-thick plates were obtained, reducing the weight by 10% as compared to the unfoamed part. Then, two series of foamed samples combined with the Core back technology were injection molded, with an enlargement of the cavity from a basic wall thickness of 3 mm up to 3.3 mm and 3.7 mm.

The solid and MuCell® foamed plates were obtained in an Arburg 570C Allrounder 2000-675 injection machine with a clamping force of 2000 kN (Arburg GmbH, Germany), whereas the IQ Foam® foamed plates were injection molded using a KraussMaffei 200-1000/390/CZ Multinject injection molding unit (KraussMaffei Group GmbH, Germany). This machine has a clamping force of 2000 kN and it is equipped with the IQ Foam®

foaming devices. In order to make a direct comparison, the same injection molding parameters were employed to produce all samples: melt temperature profile of 40-210-230-240 ºC from hopper to nozzle, injection speed of 100 cm^3 s^{-1}, mold temperature of 30 ºC and cooling time of 45 s. The shot volume for solid plates was 190 cm^3, with a holding pressure of 300 bar applied for 10 s, whereas foamed samples were injected at 165 cm3 of shot volume, and using nitrogen as blowing agent. A 0.5% content of gas was introduced at 34 bar of pressure during MuCell® processing. As the IQ Foam® equipment is only controlled by the gas pressure, which was 25 bar, the amount of gas introduced was not possible to be measured in the designed equipment.

3.2. Characterization methods

3.2.1. Morphology, apparent density and fiber distribution

After the injection procedure, the apparent density of the plates was calculated by weighing and measuring their volume. The cell structure was studied at the beginning (A), the middle (B) and the end of the flow path (C), in both parallel (MD) and transversal (TD) directions (Figure 4b) by Scanning Electron Microscopy (SEM) technique. Samples were submitted to cryogenic fracture so as to avoid altering the original morphology, and the resulting fracture surfaces were examined with a JEOL JSM-560 microscope (Jeol Ltd., Japan). Micrographs were adjusted for an appropriate level of contrast and the foam morphology was characterized by using Igor Pro® (Wavemetrics Inc., USA) and Matlab® (The MathWorks Inc., USA) software. The cell size was calculated as an equivalent diameter determined from the area of each cell, assuming a perfect spherical shape. The amount of cells per volume with respect to the non-foamed polymer is given by the cell density (N) parameter, obtained by the following equation:

$$N = \left(\frac{n}{A}\right)^{3/2} \left(\frac{\rho_s}{\rho_f}\right) \quad (1)$$

where n is the number of cells, A is the area (cm^2) of the micrograph, and ρ_s and ρ_f are the density of compact and microcellular material, respectively. The thickness of the solid skin was taken as the distance between the surface and the beginning of the foamed core. With the objective of studying variations along the molded parts, the density was also determined in samples taken from the same positions as the morphological analysis (Figure 4c).

The cell morphology and fiber orientation and distribution was assessed by Computed Tomography technique. Scans were performed at 90kV and 10W with a MultiTom Core system, (XRE bvba, Belgium), while acquisition settings were 2500 projections and an exposure time of 400 ms. All data from each sample was 3D reconstructed and filtered with RECON software from XRE and, finally, Avizo software (FEI Company, USA) was employed for materials segmentation according to their density.

The glass fiber content was measured by the determination of ash through the direct calcination method, as indicated in the ISO 3451-1 standard.

3.2.2. Mechanical properties

The specimens for mechanical tests were extracted from the rectangular plates ensuring the correspondence between the tested section and the morphology previously analyzed (Figure 4d). All tests were conducted under room temperature conditions with five samples of each set of materials. Tensile tests were made following the guidelines given in the ISO 527 standard, with 72 mm of initial clamps distance and at a crosshead speed of 50 mm min^{-1}, performing the tests on a universal testing machine Zwick/Roell Z010 (Zwick GmbH & Co. KG, Germany). Flexural tests were carried out on a Galdabini Sun 2500 (Galdabini SPA, Italy) testing machine, at a crosshead speed of 10 mm min^{-1} and a span length of 80 mm, as indicated in the ISO 178 standard.

Charpy impact tests were conducted according to the ISO 179-2 standard. A instrumented Ceast Resil impactor (Instron Ltd., UK) was employed. A 15J hammer, with a reduced mass of 3.654 kg and 0.374 m of length, was impacted at an angle of 99º, resulting in an impact rate of 2.91 m s^{-1}. The tests were performed in flatwise configuration on unnotched samples, with a span length of 62 mm.

4. RESULTS AND DISCUSSION

4.1. Morphology, apparent density and fiber distribution

The microstructure of samples injected with both MuCell® and IQ Foam® processes and extracted from the centre of the plate in MD and TD orientations as representative of the global behaviour are shown in Figure 5 and Figure 6. (The complete set of micrographs along the plate is collected in Figure S1 to Figure S4 of Supporting Information). The morphological parameters determined in MD-B and TD-B positions are summarized in Table 1 and Table 2, respectively (The extended data with the rest of analyzed sections are included in Table S1 and Table S2 of Supporting Information).

All samples exhibited a structure consisting of a solid external layers and a foamed core, which is inherent to the injection molding process. Bledzki et al. (2007) reported that the low melt strength and the semicrystalline nature of PP obstruct its foamability. However, SEM pictures exhibit a very uniform cell structure in all cases which is attributted to the fiber presence acting as heterogeneous cell nucleation agent as was firstly indicated by Colton and Suh (1987). According to this theory, the activation energy for bubble nucleation is much lower when cell sites are formed by gas trapped at the interface between polymer and filler, and then, a larger number of cells with a small size are developed in the foamed core. Additionally, glass fibers increase melt strength and thus prevent cell coalescence, improving the foamability of PP.

In melt direction (MD) micrographs depicted in Figure 5, mostly spherical cells can be observed at the starting thickness of 3 mm without using Core Back expansion. By increasing the thickness up to 3.3 mm and 3.7 mm, cells became distorted and elongated, and higher diameters were determined (see Table 1 and Table 2, as well as Table S1 and Table S2 of Supporting Information). By using the Core Back method, the cavity was volumetrically filled with the polymer/gas system, then the thickness of the mold cavity was quickly increased to a predefined extent reducing the pressure and thus enhancing cell nucleation. According to experiments carried out by Heim and Tromm (2015) with physical and chemical foaming agents and PP material, bubble nucleation occurred once the cavity is fully filled and the pressure drops due to the mold plate movement. Ahmadzai et al. (2014) explained two opposite mechanisms governing the foaming behavior in the Core Back technology. On one hand, the increased volume provides more space for foam expansion. On the other hand, the reduced pressure also induces the scape of a higher amount of gas from the polymer to the environment, lowering the portion of blowing agent for cell nucleation and growth.

According to Figure 5 and Figure 6 the former mechanism seems to be the predominant in the foamed plates of this work. Stretching forces caused by the mold opening could result in cell elongation, also accompanied by shrinkage of cell walls while polymer cooling, as stated by Heim and Tromm (2016) and Jahani et al. (2015). That is why bigger and distorted cells can be observed. Ruiz et al. (2016) also reported that cell growth continues after the Core Back movement, but most of the process is due to depressurization and mold opening. Some research works, like the ones conducted by Heim and Tromm (2012) and Spörrer and Altstädt (2007), also indicated a slightly increase in the solid skin thickness with increasing the pulling core distance. Nevertheless, qualitative and quantitative analysis in this study pointed out to unchanged or thinner layers while cavity expansion. As the thickness increased, the core region remained at the molten state for a longer time leading to thinner skin layers, as indicated by Ahmadzai et al. (2014) and Heim and Tromm (2016). The results contained in Table 1 and Table 2 (and also in Table S1 and Table S2 of Supporting Information) show an apparent density of the solid plates of around 1.04 ± 0.01 g cm^{-3}. By foaming, it was decreased by 10% without using Core Back technology. As the final thickness and overall volume increased by mold opening, the apparent density decreased up to 14% and 21% for the final thickness of 3.3 mm and 3.7 mm respectively. Despite the fact that the optimum N_2 concentration of 0.5% for mixing with crystalline materials suggested by Okamoto (2003) was employed, cell density determined in these rectangular plates were one order of magnitude lower than that of presented in previous research with square plates and the same material (Gómez-Monterde et al., 2018), because of the reduced amount of blowing agent utilized in this case. The low mold temperature used for processing the rectangular plates (30 ºC) together with the thin wall thickness could have accelerated the cooling of the polymer and hampered the nucleation, expansion and growth of a higher amount of cells.

Regarding the comparison between MuCell® and IQ Foam® injected parts, the micrographs of Figure 5 and Figure 6 illustrate well defined and uniform cell structures, which indicate that microcellular reinforced thermoplastics can be successfully developed by both foaming technologies. Slightly thicker solid skins of IQ Foam® without Core Back expansion were determined from Table 1 and Table 2. Despite the cell density measured in all samples was in the order of 10^5 cells cm^{-3}, those obtained by IQ Foam® process were slightly lower. Since the same injection molding parameters were employed for processing with both methods, differences in blowing agent dosed in each foaming process arises as the main reason for these morphological differences. Contrary to MuCell® technology, the gas in IQ Foam® process was incorporated into the polymer in pellets form. The key parameter controlling the process was the gas pressure, so the gas content injected into the polymer was not measured and cannot be directly compared. Nevertheless, a lower amount of blowing agent in the IQ Foam® molded parts is expected due to the low solubility of the nitrogen in the polymer pellets, which would explain the increased solid layer determined in the 3 mm-thick specimens, as well as the decrease in cell density. However, no differences in cell size between both processing technologies were reported, neither in Table 1 and Table 2 nor in Figure 7. From this chart it can be concluded that regardless the foaming method and combination with Core Back technology, around 90% of cells were concentrated in the range of 1 - 120 µm.

Of particular interest could be the study of the distribution and orientation of fibers in injection molded fiber-filled composites. According to the analysis carried out by Computed Tomography, fibers in the surface layer remain oriented in the direction of filling, while they appear aligned in the transversal direction in the core (Figure 8). The video included as supplementary material shows the evolution of the glass fiber orientation from the surface to the center of a MuCell® foamed sample. The same pattern is observed in all samples, regardless the process of injection molding and foaming from which were produced. Measurements of the length of the fibers provided values contained in the range of 748 ± 174 µm for all solid, MuCell® and IQ Foam® derived samples which suggested that the special machinery and conditions of the MuCell® did not affect fiber length in short-fiber reinforced thermoplastics. Fiber content remained in all specimens in the range of 20.1 ± 0.2 %.

The evolution of morphology along the part in melt direction (MD) or transversal direction (TD) yield similar values for each sample location. Solid skin tended to increase with the distance from the injection gate, whereas cell density decreased. The same behavior was also found with foamed injection molded ABS plates (Gómez- Monterde et al., 2016), and it is caused by the lower temperature of the melt at the end of the cavity end and the higher pressure of the system preventing foaming and core expansion. Tendency of cell size was inconclusive with the results obtained by analyzing SEM images.

4.2. Mechanical properties

The mechanical properties obtained from tensile, flexural and impact tests are plotted on Figure 9 (absolute and specific values of the different properties are collected in Tables S3 to S8 of Supporting Information). From the graphs it can clearly observed that foamed samples showed lower properties than the solid counterparts, because cells in the core effectively led to a reduction in density and in the effective cross-sectional area. With increasing density reduction by Core Back expansion, the reduction of both tensile and flexural modulus was nearly linear, as indicated by the closed specific values to those of solid specimens. Impact resistance decreased by around 15% when foaming without core expansion, and by 22% and 35% while increasing the thickness to 3.3 mm and 3.7 mm, respectively. That is, foamed material is more sensitive to impact loads than to tension and bending.

Concerning variations in tensile and flexural properties along the part (Tables S3 to Table S8 of Supporting Information), the mechanical properties increased with the flow length (MD-A < MD-B < MD-C), which could be attributed to a thicker solid skin formed at the end areas. The opposite trend was found in the transverse direction (TD-C < TD-B < TD-A). Results in samples taken in MD direction were higher than in TD direction, which suggests that glass fibers are preferentially oriented in the filling direction. Unlike for tensile and flexural behavior, the impact resistance at the end of areas of the cavity experienced an increase for both testing directions (MD and TD), suggesting that there is a greater dependency on the surface skin layer than upon fiber orientation. Additionally, differences in MD and TD of impact resistance values of solid samples were around 28%, but they were significantly reduced by foaming and Core Back expansion molding, reaching a deviation between both directions of 5% when the thickness was raised up to 3.7 mm.

In reference to the comparison between foaming technologies, tensile and flexural modulus of samples obtained by IQ Foam® process were higher and differed from the corresponding ones to MuCell® by approximately 10%. The impact resistance was the property with less differences between both foaming technologies, around 7%. The thicker solid skins seems to be the most likely reason for this higher results obtained with the IQ Foam® samples. On the basis of the lower blowing agent incorporated in the IQ Foam® plates, the consequent reduction in cell density led to wider cell struts and higher effective bearing area able to withstand higher mechanical loads. These differences between foamed samples through both processes were lowered when Core Back was applied and the volume cavity was increased, which suggests that, as the part gets thicker, the mechanical properties became more dependent on apparent density and the overall thickness than upon skin thickness and cell density.

Of particular interest is the analysis of the flexural behavior of plastic foams when employing the Core Back expansion molding process. For engineering purposes, design criteria is based on the flexural stiffness rather than on the flexural modulus. This parameter involves the geometry of the part by means of the moment of inertia. For flat panel geometries, the flexural stiffness (S_f) is calculated as follows:

$$S_f = E_f I = E_f \frac{bh^3}{12} \tag{2}$$

In Equation 2, I is the moment of inertia, E_f is the flexural modulus and b and h the part width and thickness, respectively. Thus, flexural stiffness is significantly increased by the third power of the thickness. Figure 10 illustrates the evolution of the relative, specific flexural strength by foaming and increasing the thickness with Core Back technology. It is worth to notice that despite the drop in flexural modulus, the stiffness can be improved up to 200% as compared to that of the solid counterpart by increasing the thickness to 3.7 mm. A global comparison of the mechanical properties and morphological characteristics between samples made with the two processes has been summarized in the multivariable plot of Figure 11. By using a minimum amount of blowing agent with the IQ Foam® technology, foamed plastic parts obtained through IQ Foam® exhibited thicker solid skins and lower cell densities, but consequently higher mechanical properties. Additional benefits such as cost-effectiveness, easy-operation and machine-independence enable IQ Foam® to produce lightweight parts with comparable properties to that of the MuCell® technology, but also with a reduced economic investment and a simplified control.

5. CONCLUSIONS

Although thermoplastic foams have been used in different structural applications for a long time, their potential capabilities are still far from being exhausted. The increasing demand for lightweight, optimized and economized automotive products calls for new solutions in the injection molding industry. In this work, the complementary Core Back tool technology and a new foaming injection molding process named IQ Foam® have been evaluated and compared to the already known MuCell®. The analysis of the cell structure and mechanical behavior of injection molded plates made of PP 20GF through both technologies and with two expansion ratios of the thickness by the Core Back technique led to the following conclusions:

- By pulling the core and increasing the final thickness of the part with the Core Back tool process, the apparent density decreased, solid skins got thinner but cells became bigger. Absolute mechanical properties decreased with the apparent density but specific ones remained close to that of the solid material. Furthermore, design criteria parameters such as the bending stiffness were greatly enhanced due to the build-up in the overall thickness.
- The new foaming technology IQ Foam® arises as an alternative foaming technology able to produce microcellular parts with comparable properties to those manufactured by MuCell® process. By using a minimum content of blowing agent, the number of nucleated cells was reduced and a thicker solid skin was formed, which led to slightly higher mechanical properties. Some additional benefits are the possibility to be used in any conventional injection molding machine, easy operation and low economical investment required.

ACKNOWLEDGEMENTS

The authors are grateful to the Research Lab of Covestro AG (Leverkusen, Germany) and the Institut für Recycling of the Ostfalia Hochschule (Wolfsburg, Germany) for their cooperation with the injection molding experiments; to the CORELAB laboratory of the Universitat de Barcelona for for their analysis through the Computed Tomography technique; as well as to the Ministerio de Economía y Competitividad from Spain for the MAT2013-40730P and MAT2016-80045R projects.

REFERENCES

Ahmadzai, A., Behravesh, A.H., Sarabi, M.T., Shahi, P., 2014. Visualization of foaming phenomena in thermoplastic injection molding process. J. Cell. Plast. 50, 279-300.

Bledzki, A.K., Faruk, O., Kirschling, H., Kühn, J., Jaszkiewicz, A., 2007. Microcellular polymer and composites. Part II. Properties of different types of microcellular materials. Polimery-W. 52, 3-12.

Colton, J.S., Suh, N.P., 1987. The nucleation of microcellular thermoplastic foam with additives: Part I: Theoretical considerations. Polym. Eng. Sci. 27, 485-492.

Elduque, D., Claveria, I., Fernandez, A., Javierre, C., Pina, C., Santolaria, J., 2014. Analysis of the Influence of Microcellular Injection Molding on the Environmental Impact of an Industrial Component. Adv. Mech. Eng. 6, 793269.

Gómez-Monterde, J., Sánchez-Soto, M., Maspoch, M.L., 2018. Microcellular PP/GF composites: Morphological, mechanical and fracture characterization. Compos. Part A-Appl. S. 104, 1-13.

Gómez- Monterde, J., Sánchez- Soto, M., Maspoch, M.L., 2018. Influence of injection molding parameters on the morphology, mechanical and surface properties of ABS foams. Adv. Polym. Tech. doi:10.1002/adv.21944.

Gómez- Monterde, J., Schulte, M., Ilijevic, S., Hain, J., Sánchez- Soto, M., Santana, O.O., Maspoch, M.L., 2016. Effect of microcellular foaming on the fracture behavior of ABS polymer. J. Appl. Polym. Sci. 133, 43010.

Hain, J., 2015. Thermoplastschaum-Spritzguss - neue Möglichkeiten durch IQ-Foam. Kunstofftrends im Automobil Conference. Wolfsburg (Germany).

Hamidinejad, M., Zhao, B., Chu, R.K.M., Moghimian, N., Naguib, H.E., Filleter, T., Park, C.B., 2018a. Ultralight Microcellular Polymer–Graphene Nanoplatelet Foams with Enhanced Dielectric Performance. ACS Appl. Mater. Interfaces. 10, 19987-19998.

Hamidinejad, M., Zhao, B., Zandieh, A., Moghimian, N., Filleter, T., Park, C.B., 2018b. Enhanced Electrical and Electromagnetic Interference Shielding Properties of Polymer–Graphene Nanoplatelet Composites Fabricated via Supercritical-Fluid Treatment and Physical Foaming. ACS Appl. Mater. Interfaces. 10, 30752-30761.

Handschke, A., Mitzler, J., 2012. Physical Foaming Made Very Easy. Kunsts.-Plast. 10, 151-156.

Heim, H.-P., Tromm, M., 2012. Pull and Foam – Method: Partially Foamed Components – First Investigations With Chemical and Physical Blowing Agents. Annual Technical Conference - ANTEC: Society of Plastics Engineers (SPE). Orlando (USA).

Heim, H.-P., Tromm, M., 2015. General aspects of foam injection molding using local precision mold opening technology. Polymer. 56, 111-118.

Heim, H.-P., Tromm, M., 2016. Injection molded components with functionally graded foam structures – Procedure and essential results. J. Cell. Plast. 52, 299-319.

A.T.Kearny, 2012. http://www.atkearney.com/chemicals/article?/a/plastics-the-future-for-automakers-and-chemical-companies

Jahani, D., Ameli, A., Saniei, M., Ding, W., Park, C.B., Naguib, H.E., 2015. Characterization of the Structure, Acoustic Property, Thermal Conductivity, and Mechanical Property of Highly Expanded Open-Cell Polycarbonate Foams. Macromol. Mater. Eng. 300, 48-56.

Kim, H.C., Wallington, T.J., 2013. Life-Cycle Energy and Greenhouse Gas Emission Benefits of Lightweighting in Automobiles: Review and Harmonization. Environ. Sci. Technol. 47, 6089-6097.

Kuang, T., Chang, L., Chen, F., Sheng, Y., Fu, D., Peng, X., 2016. Facile preparation of lightweight high-strength biodegradable polymer/multi-walled carbon nanotubes nanocomposite foams for electromagnetic interference shielding. Carbon. 105, 305-313.

Kuang, T., Chen, F., Chang, L., Zhao, Y., Fu, D., Gong, X., Peng, X., 2017a. Facile preparation of open-cellular porous poly (l-lactic acid) scaffold by supercritical carbon dioxide foaming for potential tissue engineering applications. Chem. Eng. J. 307, 1017-1025.

Kuang, T., Ju, J., Yang, Z., Geng, L., Peng, X., 2018. A facile approach towards fabrication of lightweight biodegradable poly (butylene succinate)/carbon fiber composite foams with high electrical conductivity and strength. Compos. Sci. Technol. 159, 171-179.

Kuang, T., Li, K., Chen, B., Peng, X., 2017b. Poly (propylene carbonate)-based in situ nanofibrillar biocomposites with enhanced miscibility, dynamic mechanical properties, rheological behavior and extrusion foaming ability. Compos. Part B-Eng. 123, 112-123.

Min, Z., Yang, H., Chen, F., Kuang, T., 2018. Scale-up production of lightweight high-strength polystyrene/carbonaceous filler composite foams with high-performance electromagnetic interference shielding. Mater. Lett. 230, 157-160.

Okamoto, K.T., 2003. Microcellular Processing, first ed. Hanser Publishers, Cincinnati, pp. 186.

Pantani, R., Volpe, V., Titomanlio, G., 2014. Foam injection molding of poly(lactic acid) with environmentally friendly physical blowing agents. J. Mater. Process. Tech. 214, 3098-3107.

Pierick, D.E., Anderson, J.R., Sung, W.C., Chen, L., Stevenson, J.F., Laing, D.E., 2005. Injection molding of polymeric material. US Patent US6884823 (B1). United States.

Pierick, D.E., Anderson, J.R., Sung, W.C., Stevenson, J.F., Laing, D.E., 1999. Injection molding of microcellular material. European Patent EP0952908 (A2). Europe.

PlasticPortal, 2014. http://www.plasticportal.eu/en/thermoplastic-foam-injection-molding/c/2416

Ruiz, J.A.R., Vincent, M., Agassant, J.F., 2016. Numerical Modeling of Bubble Growth in Microcellular Polypropylene Produced in a Core-Back Injection Process Using Chemical Blowing Agents. Int. Polym. Proc. 31, 26-36.

Sánchez-Soto, M., Gordillo, A., Arasanz, B., Aurrekoetxea, J., Aretxabaleta, L., 2006. Optimising the gas-injection moulding of an automobile plastic cover using an experimental design procedure. J. Mater. Process. Tech. 178, 369-378.

Schütz, C., Hain, J., Müller, M., 2015. System zum Schleusen, Dosieren und Spritzgiessen von Material. German Patent DE102014212048 (A1). Germany.

Spörrer, A.N.J., Altstädt, V., 2007. Controlling Morphology of Injection Molded Structural Foams by Mold Design and Processing Parameters. J. Cell. Plast. 43, 313-330.

Xu, J., 2010. Microcellular Injection Molding, first ed. John Wiley & Sons, Hoboken, pp. 618.

FIGURE CAPTIONS

Figure 1. Plant concept for MuCell® process. Modified from PlasticPortal (2014).

Figure 2. Plant concept for IQ Foam® process. Modified from PlasticPortal (2014).

Figure 3. Operating steps of IQ Foam® technology.

Figure 4. Schematic representation of **a)** injection molded plates; and samples extracted for **b)** density measurements, direct calcination test, and CT scans; **c)** morphological analysis; **d)** mechanical testing.

Figure 5. SEM micrographs of MuCell® and IQ Foam® foamed plates taken in MD-B position.

Figure 6. SEM micrographs of MuCell® and IQ Foam® foamed plates taken in TD-B position.

Figure 7. Cell size distribution in MD-B position of PP 20GF foamed plates with **a)** MuCell®; **b)** IQ Foam®.

Figure 8. Fiber orientation patterns of solid and foamed parts obtained by Computed Tomography.

Figure 9. a) Tensile modulus; **b)** flexural modulus; **c)** impact resistance of solid and foamed samples.

Figure 10. Relative, specific flexural stiffness (S_f) evolution with density reduction and thickness increase.

Figure 11. Multivariable plot comparing morphological characteristics and mechanical properties of solid, MuCell® and IQ Foam® foamed specimens.

TABLES

Table 1. Morphological parameters in MD-B section of MuCell® and IQ Foam® foamed PP 20GF plates.

Condition No.	Section	Density (g cm^{-3})	Skin thickness (mm)	Cell density (cells cm^{-3})	Cell size range (µm)
MuCell® 3 mm	MD-B	0.94 ± 0.01	0.41	$7.1 \cdot 10^5$	9-165
MuCell® / Core Back 3.3 mm	MD-B	0.90 ± 0.01	0.46	$8.4 \cdot 10^5$	9-263
MuCell® / Core Back 3.7 mm	MD-B	0.82 ± 0.01	0.41	$6.1 \cdot 10^5$	4-286
IQ Foam® 3 mm	MD-B	0.94 ± 0.01	0.70	$4.4 \cdot 10^5$	6-195
IQ Foam® / Core Back 3.3 mm	MD-B	0.90 ± 0.01	0.41	$4.5 \cdot 10^5$	4-234
IQ Foam ® / Core Back 3.7 mm	MD-B	0.82 ± 0.01	0.40	$5.5 \cdot 10^5$	3-276

Table 2. Morphological parameters in TD-B section of MuCell® and IQ Foam® foamed PP 20GF plates.

Condition No.	Section	Density (g cm^{-3})	Skin thickness (mm)	Cell density (cells cm^{-3})	Cell size range (μm)
MuCell® 3 mm	TD-B	0.94 ± 0.01	0.42	$8.5 \cdot 10^5$	9-125
MuCell® / Core Back 3.3 mm	TD-B	0.90 ± 0.01	0.38	$8.2 \cdot 10^5$	9-223
MuCell® / Core Back 3.7 mm	TD-B	0.82 ± 0.01	0.31	$6.8 \cdot 10^5$	3-280
IQ Foam® 3 mm	TD-B	0.94 ± 0.01	0.67	$4.3 \cdot 10^5$	9-128
IQ Foam® / Core Back 3.3 mm	TD-B	0.90 ± 0.01	0.42	$5.8 \cdot 10^5$	7-222
IQ Foam ® / Core Back 3.7 mm	TD-B	0.81 ± 0.01	0.32	$6.8 \cdot 10^5$	3-288

Figure 1

Click here to download high resolution image

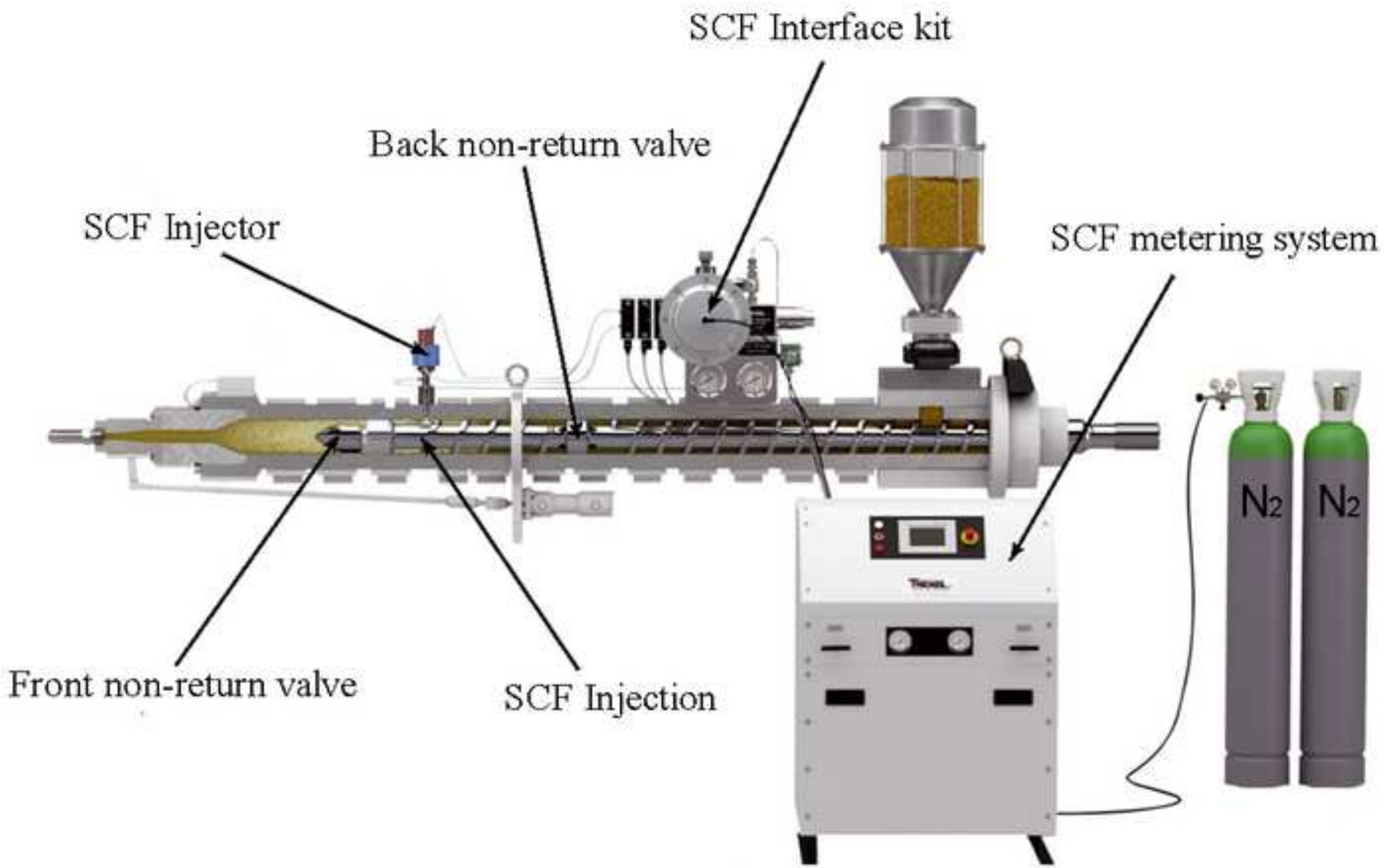
SCF Interface kit
Back non-return valve
SCF Injector
SCF metering system
Front non-return valve
SCF Injection
N2
N2

Figure 2

Click here to download high resolution image

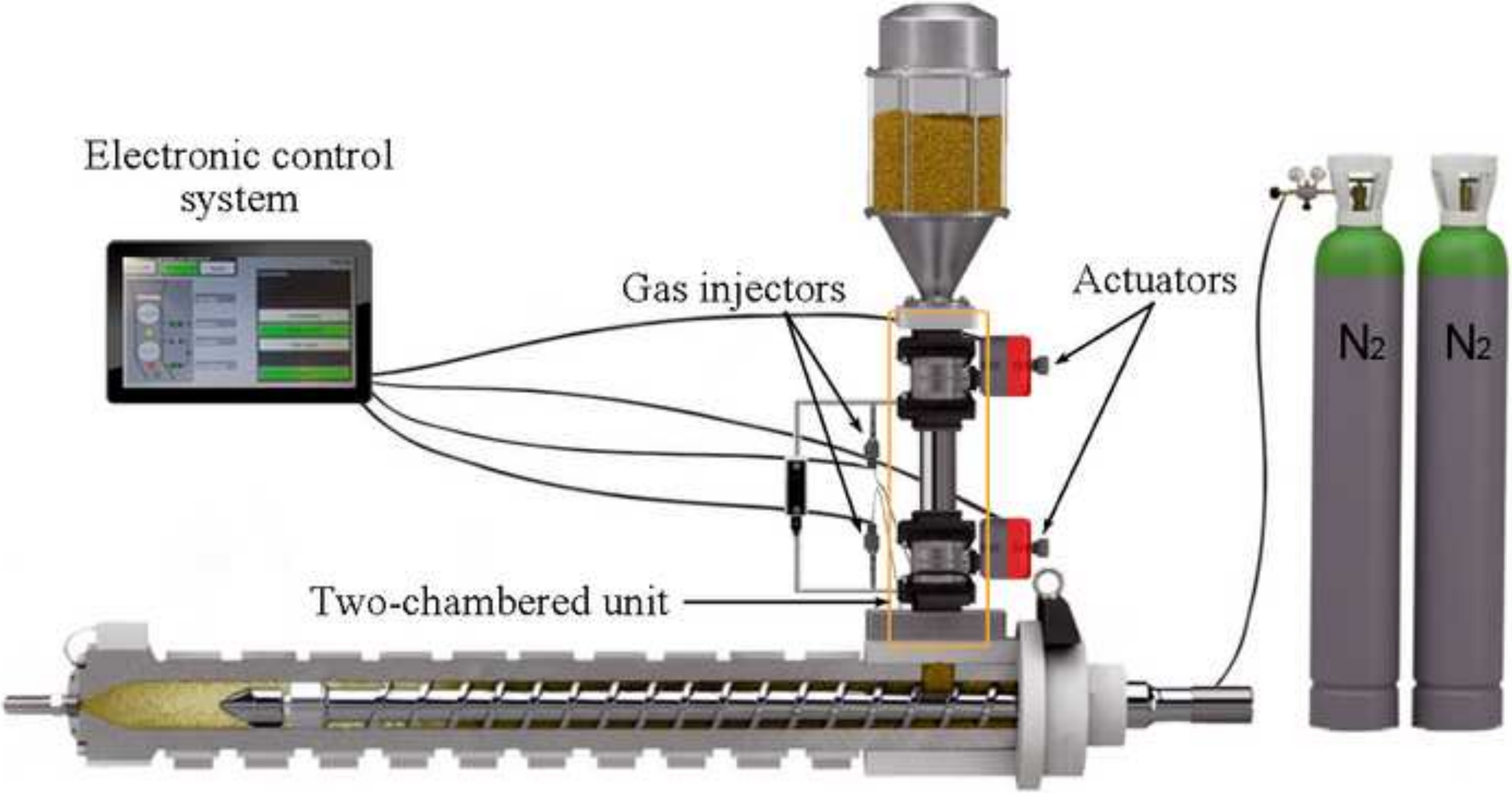

Electronic control system
Gas injectors
Actuators
Two-chambered unit
N2
N2

Figure 3

Click here to download high resolution image

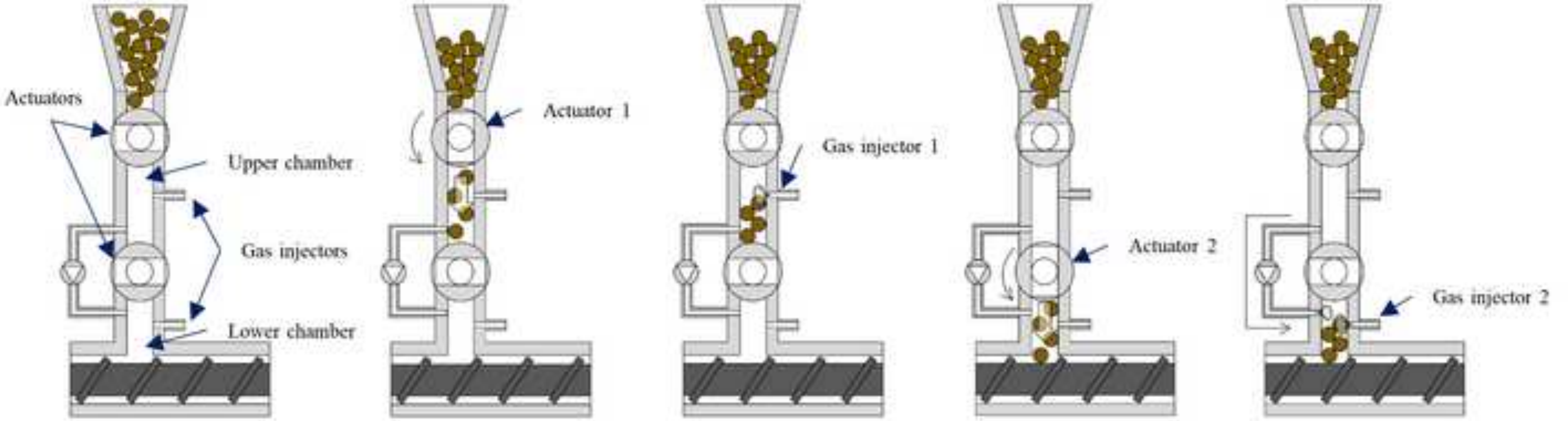
Actuators
Upper chamber
Gas injectors
Lower chamber
Actuator 1
Gas injector 1
Actuator 2
Gas injector 2

1. Chambers closed. No feeding.

2. Actuator 1 opens and pellets fall into the upper chamber.

3. Injector 1 introduces gas into the upper chamber.

4. Actuator 2 opens and pellets fall into the lower chamber.

5. Gas is rerouted from upper to lower chambers. Injector 2 introduces gas to keep the pressure.

Figure 4

Click here to download high resolution image

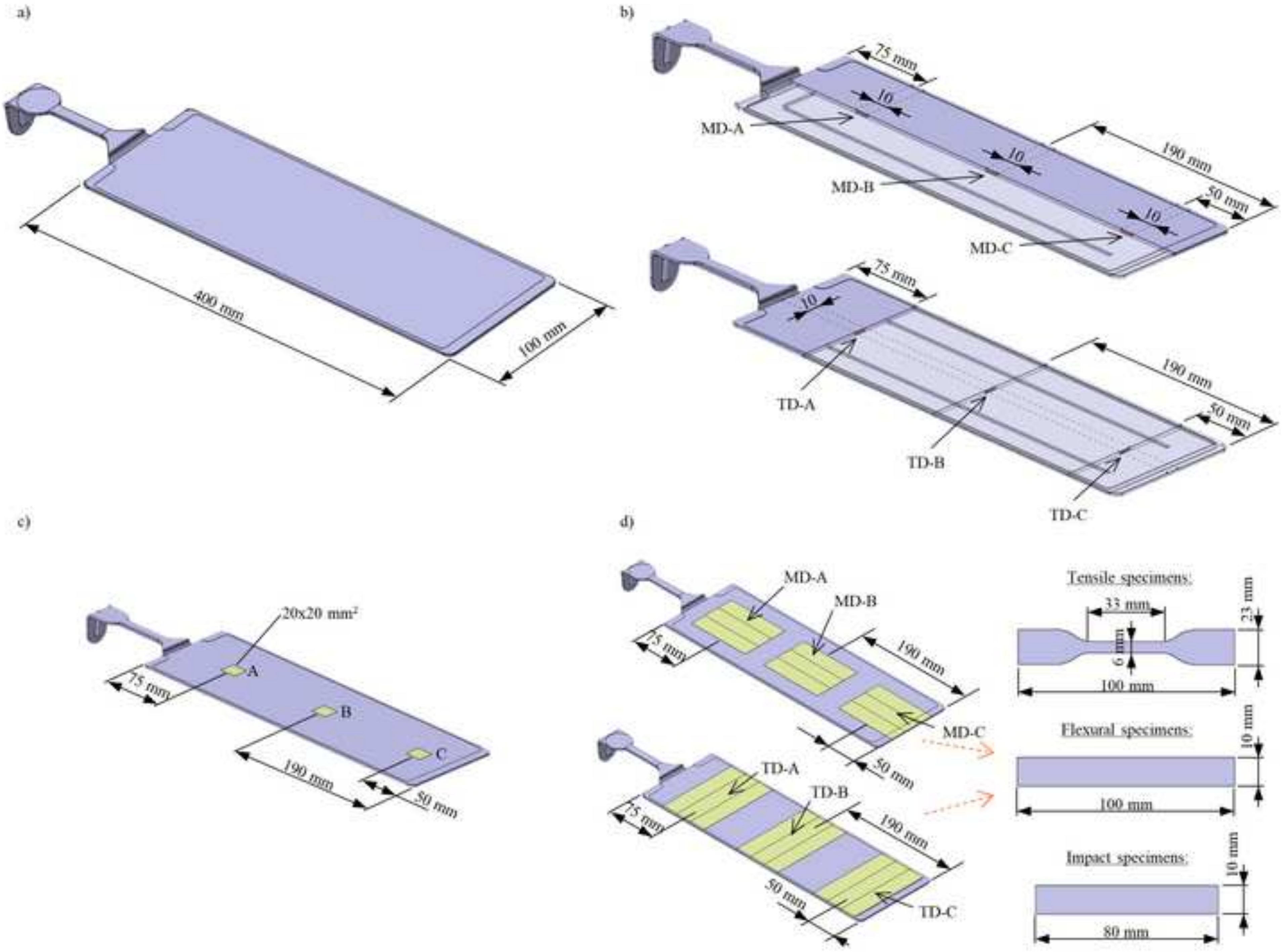
a)
400 mm
100 mm
b)
75 mm
10
10
10
MD-A
MD-B
MD-C
190 mm
50 mm
75 mm
10
TD-A
TD-B
TD-C
190 mm
50 mm
c)
20x20 mm²
A
B
C
75 mm
190 mm
50 mm
d)
MD-A
MD-B
MD-C
75 mm
190 mm
50 mm
TD-A
TD-B
TD-C
75 mm
190 mm
50 mm
Tensile specimens:
33 mm
6 mm
23 mm
100 mm
Flexural specimens:
10 mm
100 mm
Impact specimens:
10 mm
80 mm

Figure 5

Click here to download high resolution image

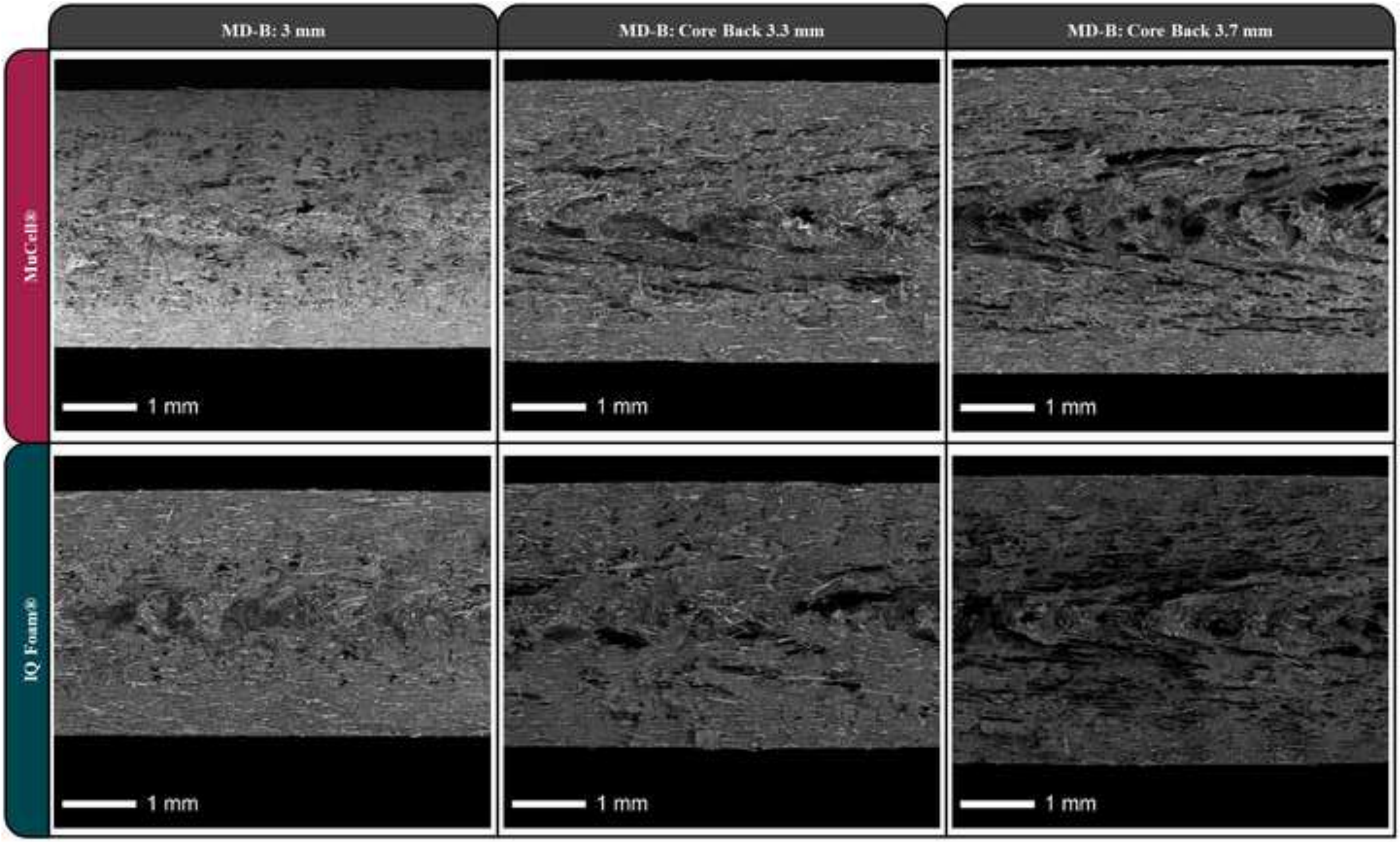
MD-B: 3 mm
MD-B: Core Back 3.3 mm
MD-B: Core Back 3.7 mm
MuCell®
IQ Foam®
1 mm
1 mm
1 mm
1 mm
1 mm
1 mm

Figure 6

Click here to download high resolution image

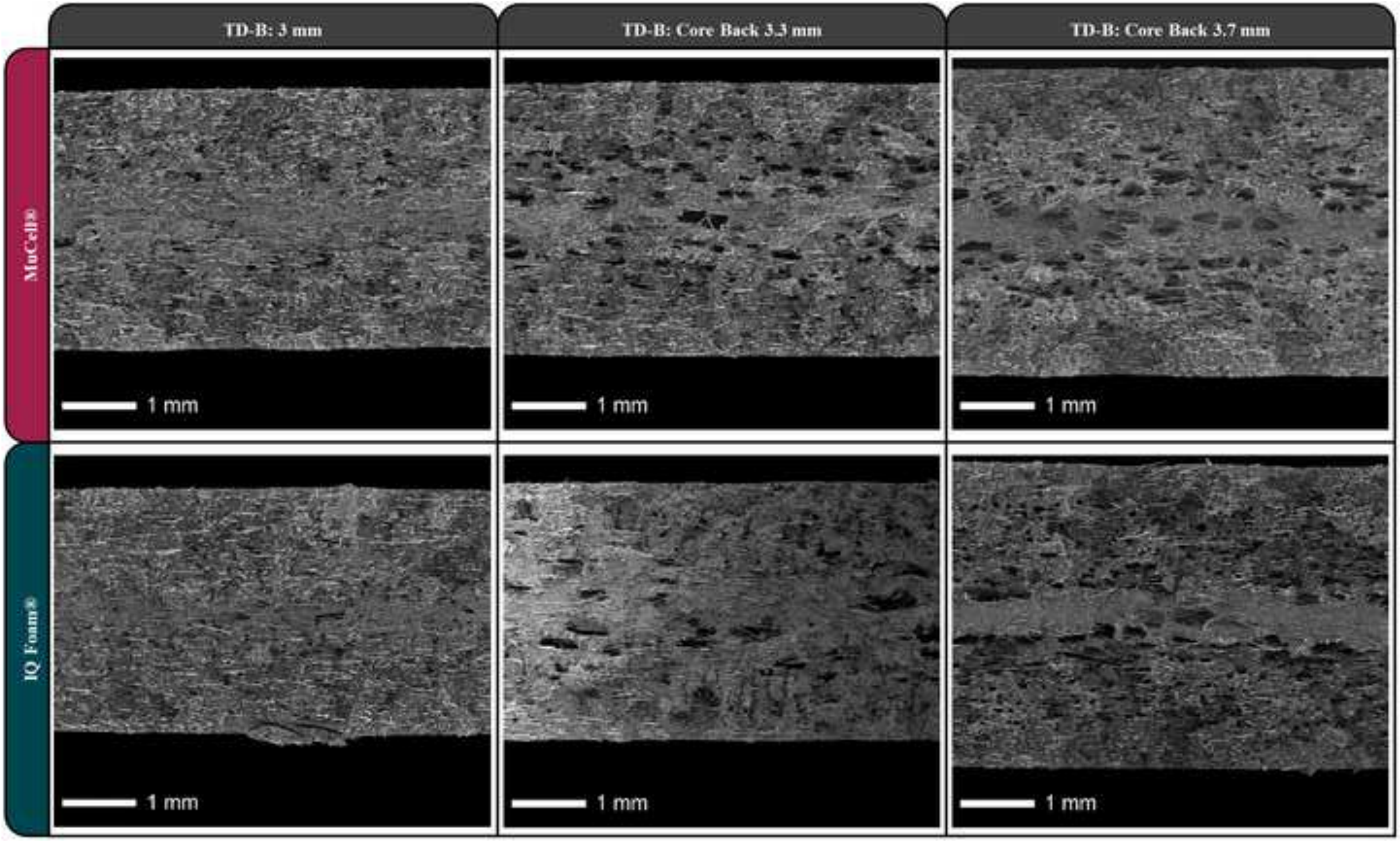
TD-B: 3 mm
TD-B: Core Back 3.3 mm
TD-B: Core Back 3.7 mm
MuCell®
IQ Foam®
1 mm
1 mm
1 mm
1 mm
1 mm
1 mm

Figure 7

Click here to download high resolution image

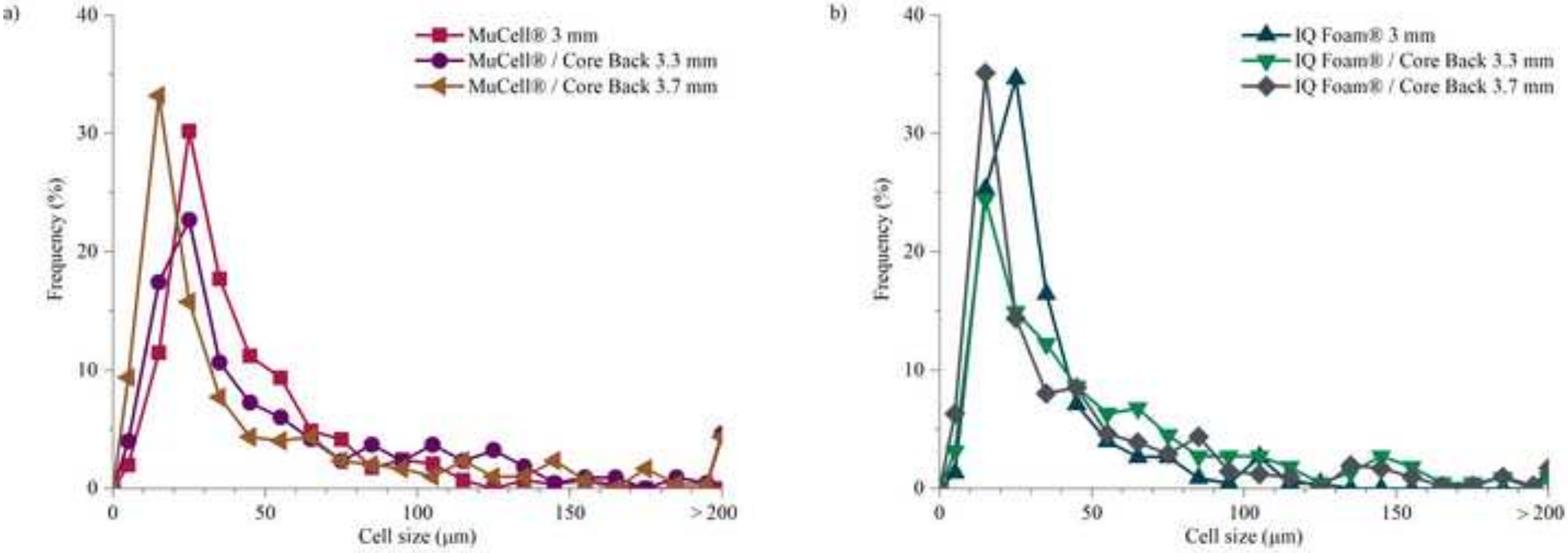

Figure 8

Click here to download high resolution image

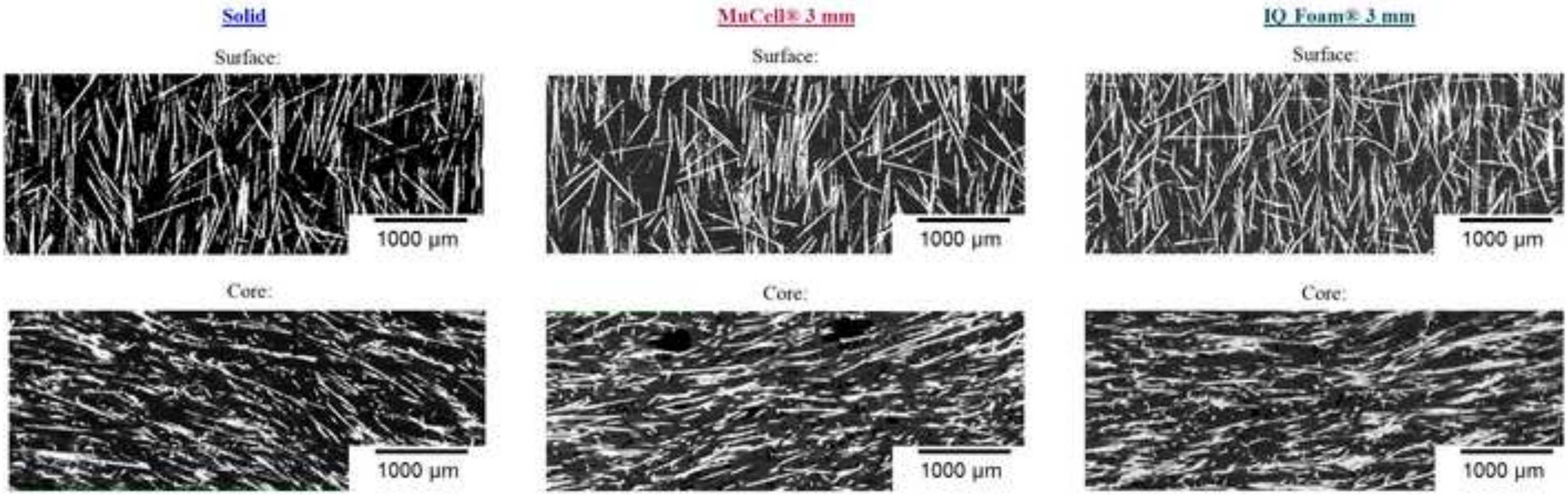
Solid
MuCell® 3 mm
IQ Foam® 3 mm
Surface:
Surface:
Surface:
1000 µm
1000 µm
1000 µm
Core:
Core:
Core:
1000 µm
1000 µm
1000 µm

Figure 9

Click here to download high resolution image

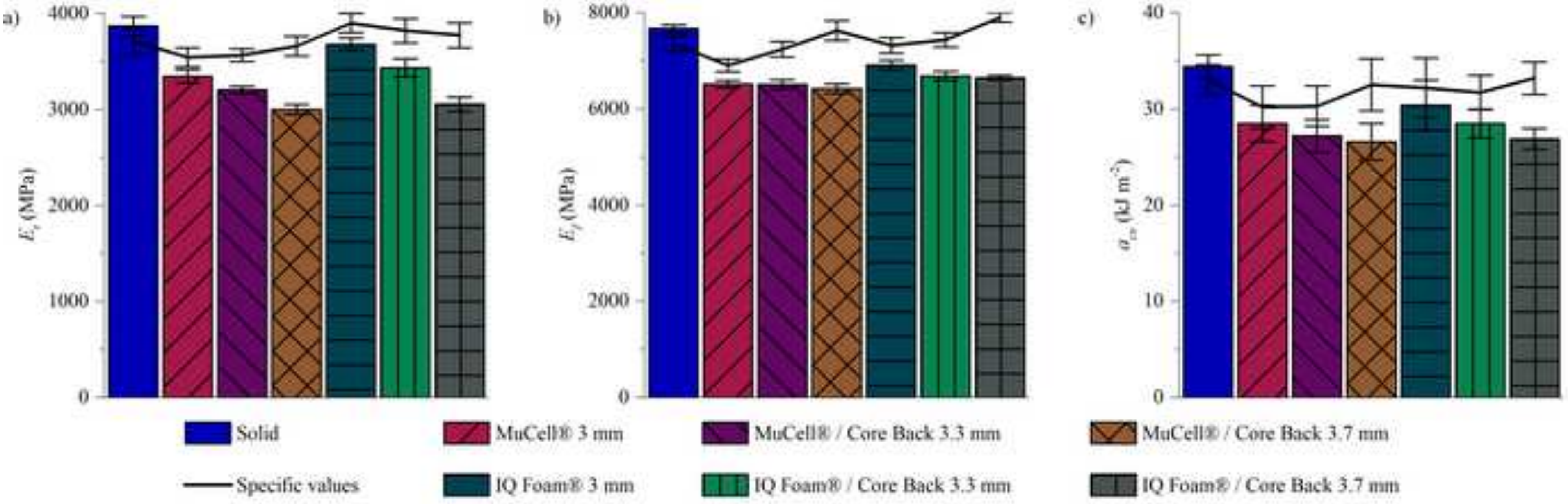

Figure 10

Click here to download high resolution image

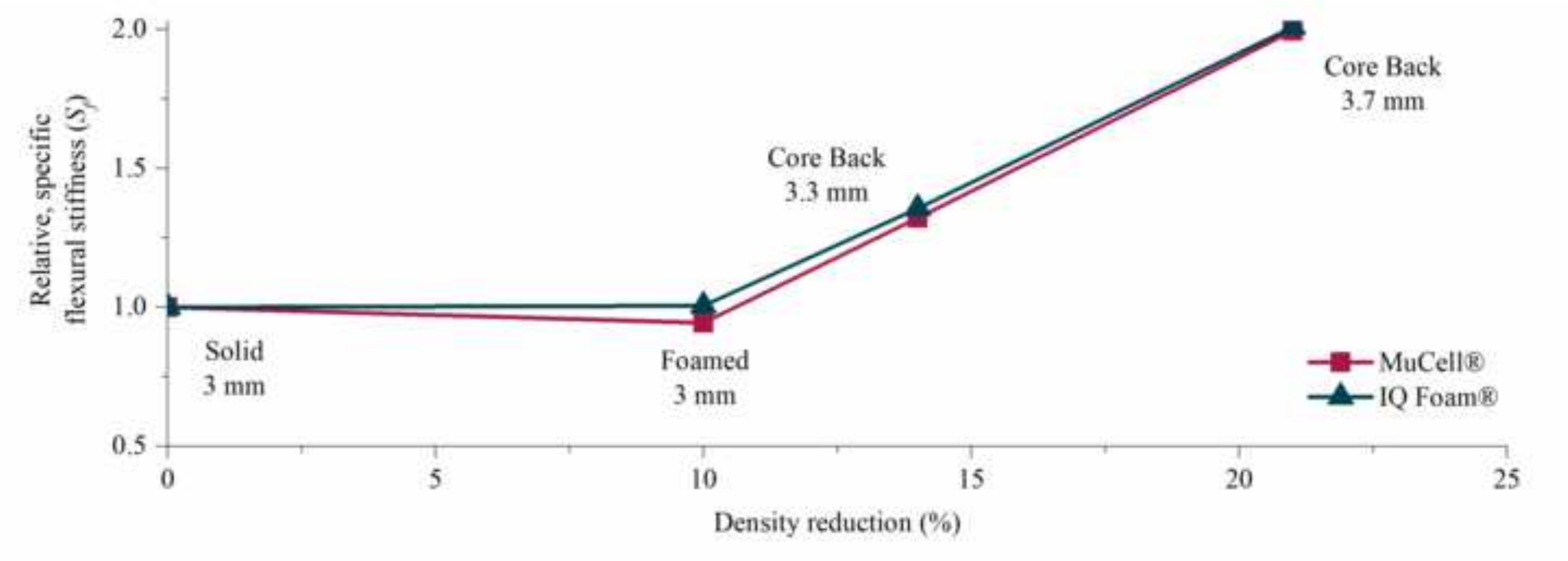

Figure 11

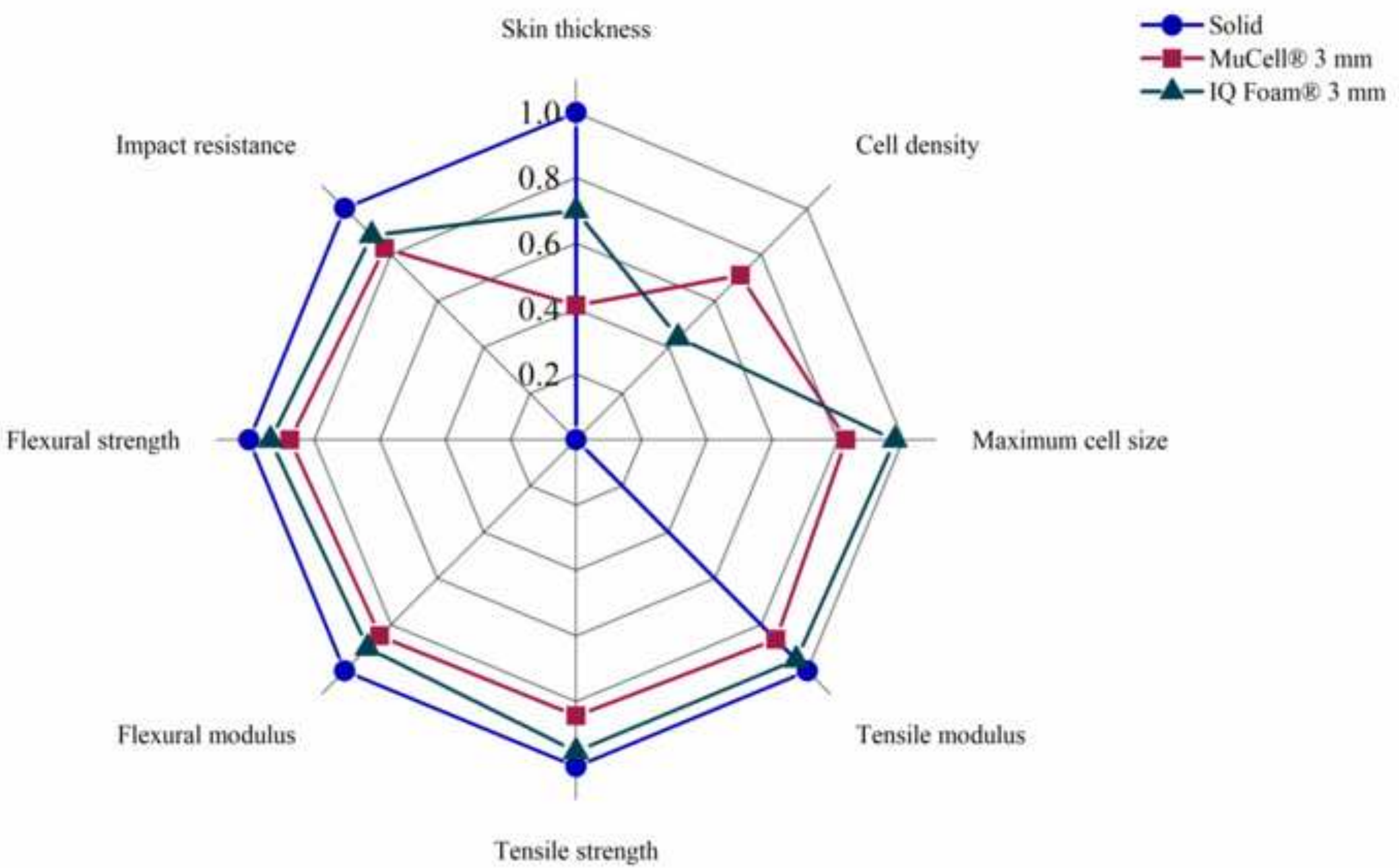Click here to download high resolution image